

**FREQUENCY DOMAIN BASED AUTOMATIC SOT WELDING DEFECT DETECTION****D. JEYASIMMAN<sup>a1</sup> AND GOVINDAN VENUGOPAL<sup>b</sup>**<sup>ab</sup>Periyar Maniammai University, Periyar Nagar, Vallam, Thanjavur, Tamilnadu, India**ABSTRACT**

**In this paper, ultrasonic resound signs of four sorts of stainless steel resistance spot welds, to be specific fizzled weld, stick weld, great weld, and flawed weld with gas pore, are dissected in the time space, recurrence area, and time-recurrence space in light of Discrete cosine transform (DCT) coefficient change. Fourteen ultrasonic trademark signals which can mirror the various types of spot welds are removed and can be naturally recognized and arranged by back-engendering (BE) neural system. The technique for this paper can understand the shrewd ID of resistance spot welding absconds, and the practicality of this strategy has been checked in the experiment**

**KEYWORDS:** Spot welding; Crack detection; Ultrasonic signals; Thermography

Quality inspection at the end of the production line is an important milestone in the industry, especially for high-performance components. Parts undergo strong mechanical and thermal stress should be carefully checked, in which small defects can affect the performance and reliability components. Crack detection is one of the most common observations to be made, because the cracks are a common source of failure, and they affect a large number of different production.

For metal parts, crack detection is still performed utilizing a technology called "magnetic particle inspection" (MPI), the part to be analyzed is washed, then put into a magnetic field and finally covered with magnetic particles, either in the form of a powder, or, more often, in a wet suspension. Cracks are easily detected because they cause leakage of magnetic flux; Such leaks are reinforced by particles, which can be viewed using UV light. The whole process is very complex and must be done manually; it is also very time consuming, the parts must be cleaned, magnetized, covered with particles, inspected, de-magnetized and clean again. Moreover, magnetic particles and the carrier are their source of pollution, and should be properly processed after use.

**STATE OF THE ART**

The topic of crack detection has been managed in many different ways in the literature, given the strong importance of this type of quality. A variety of methods have been used, as the propagation of ultrasound is used in [Gachagan et.al., 2004] to detect cracks and lamination defects in metal tubes, or eddy currents [Theodoulidis et.al., 1994, Xu and Shida 2008, Tian et.al., 2005]. The use of other utilizing magnetic camera to detect a crack in

the parts that are at high temperatures [Hwang et.al., 2009], or magnetic flux leakage [Sophia et.al., 2006], but the method described in [Liu, 2007] study, the heat produced by a Joule -hrifum.

Methods based on the analysis model has also been exploited in literature, from the analysis of welding defects in pipelines [Shafeek et.al., 2004] concrete surface analysis [Prasanna et.al., 2012] and the protection of cultural heritage [Turakhia et.al., 2012]. Thermographic image analysis systems have recently been proposed to deliver in situ non-destructive inspections of thermo-mechanical fatigue test [Genest et.al.,]; system showed high sensitivity to be able to detect cracks smaller than 500 nm. The system proposed in [Wagner et.al., 2010] is slightly different from the others discussed above and it is meant to see the different types of materials for testing fatigue, and detect cracks as soon as they appear.

Thermography based crack detection is often combined with stimulation methods like eddy currents [Kostson et.al.,] or laser beams; in particular, lasers provide the inspection process with high flexibility, as it can concentrate heat in a small place, and makes and turn off the heat source can be done instantly, creating pulses at high frequency. This last characteristic is utilized in pulse thermography and methods derived from it [Maldague et.al., 2002]. Another method is based on laser technology is "flying spot active thermography" [Maffren, et.al.], which refers to the laser spot causes local activation by the inspection. This is similar to the analysis method used in ThermoBot project, and was selected in [Maffren, et.al.] for a high pressure turbine blades.

The following two methods to detect cracks in metal parts will be described. They were developed to

handle the task of automated crack detection of objects with different characteristics and different methods of heat stimulation. Both smooth and rugged metal parts must be considered, excited by both pulsed and continuous heat.

**ANALYSIS**

Parts that were considered for testing control systems belong to two categories:

- Test Part A: metal plate, which consists of eight sheets of smooth reflecting metal;
- Test Part B: portions of the crankshaft, the rugged metal, and are characterized by complex geometry.

Even though both test parts are metal and physical principle of detection is based is the same for both acquired pictures are very different, because different work surfaces.

Test part A is the simplest case: a flat mirror-like surface provides highly uniform images, which are easy to work. A laser beam which strikes the part saturates the camera, and appears as a white spot surrounded by gray areas declining, due to the heat flow from the hot spot. The crack detection algorithm for smooth metal parts such as test Part A is based on the analysis of the area where the heat is distributed.

Analysis of heat flow area is made in three steps:

- Hot Spot detection,
- Radial gradient analysis,
- Inclined analysis.

As a first step, the hot spot needs to be detected. This is fairly easy and laser spot is part of the image with the highest temperature, and is always saturated in all working conditions of the place. It is also reasonable to assume that this is true in most of the acquisition structure, the hot spot detection is carried out with a simple algorithm. A dynamic threshold, after the lowest and the highest temperature values found in the film, is first applied to get the binary image laser spot is one white element. A dilation operator is then used to smooth shape Goals; hub is finally rated as the center of mass resulting shape.

When the shape and location of the laser spot is available it is possible to distinguish the surrounding area to perform crack detection.

**Radial Gradient**

The primary analysis includes the thermal motion of the area is moved to its radial gradient. While normal gradient pixel difference operator considers only along horizontal and vertical axes, radial version considers many directions intersecting the central point, which corresponds to the hot spot center of gravity in our case.

The radial gradients are usually evaluated by comparing items that are aligned along a certain direction intersecting the center. But when this is assessed in a single domain model, important side effect should be considered: the number of pixels in a given distance to the center is not constant but depends on the distance itself. This is important in a differential, for example, in [Jacquey et.al., 2007] approach is proposed that instead of comparing pixels focuses on image areas of variable size, depending on the distance to the center.

Our approach to the problem is slightly different, and moves from the outer region toward the center. Consider the picture portion of FIG. 3 (left): the center is represented by a green spot on the bottom left corner. For each pixel, vector connecting it to the center is shown, the color is red if it exceeds only one pixel, and a blue mark if points are two. It is important to understand the two issues that pixels with red vector can be compared with the second pixel (indicated by the vector), as it happens in other deficit Evaluation. Notes with blue vector must be compared to more than one other pixel, ie two that are cut by a vector pointing to the center, as indicated in Fig. 3 (middle). As it can be seen in the picture, each pixel in the image is based on no more than two other pixels,

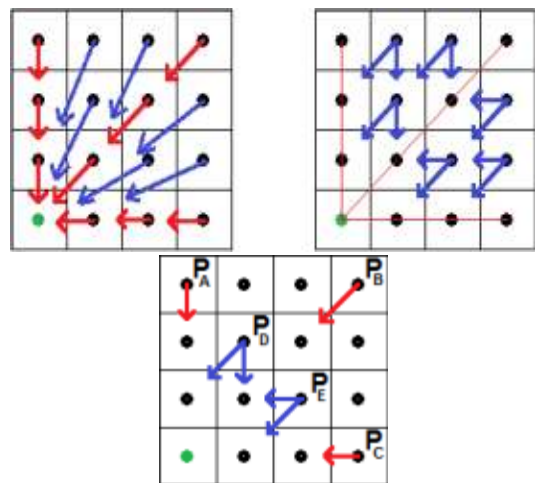


Figure 1: The radial gradient systems.

The method described above, four different conditions can be recognized, in short, in Figure 3 (right). Pixels PA, PB and PC are connected to the center along a vertical, diagonal and horizontal respectively; For this reason, the radial gradient is evaluated by comparing them with one frumdilsins is that indicated by the vector. In the case of PD, the line connecting the center of the image has a higher vertical component: PD should be compared with the pixels placed along the left and down directions. PE issue is impressive. The values of the radial gradient will be therefore:

$$P_A' = P(X_A, Y_A + 1) - P_A$$

$$P_B' = P(X_B - 1, Y_B + 1) - P_B$$

$$P_C' = P(X_C - 1, Y_C) - P_C$$

$$\frac{P(X_D - 1, Y_D + 1) - P(X_D, Y_D + 1)}{P_D} = f$$

$$\frac{P(X_E - 1, Y_E) - P(X_E - 1, Y_E + 1)}{P_E} = f$$

where  $P(X, Y)$  is the point of coordinates  $(X, Y)$  and  $f()$  is a function that manages different weighting neighboring pixels.

**Inclined**

The tangential gradient provides additional information with respect to the radial version, it is important to fully describe the area around the laser spot. The principle that ranking is similar to that described for a radial gradient, with one fundamental exception that in this case the vectors are not the policy of linking each pixel instead of the center, but are contrary to such policies. The program in Fig. 5 has the meaning shown in Fig. 4 in this new context.

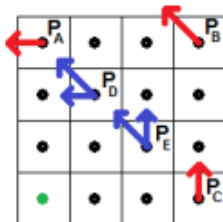


**Figure 2: Four types of pixel comparisons interfacing gradient algorithm.**

**Radial Deficiency**

Deficits assessed the area around the laser spot is not uniform, and it is higher in the places covered site, as it is easy to understand by examining the heat transmission inside metal parts. From editing standpoint, this breaks the uniformity of the area being viewed, and therefore should be the opposite. To balance this effect, we suggest a correction called radial deficiency (RGE), which is funding the deficit depends on the distance to the central laser spot. The equalization is applied to the area around the laser spot where the maximum length defined by the parameter  $L_{MAX}$ . The amplification is defined as a function of distance to middle- and increase linearly repealed  $G_{MIN}$  where a certain value  $G_{MAX}$  which is reached at a distance  $L_{LIM}$ , Then get Feeds:

$$RGE(l) = \begin{cases} G_{MIN} + \alpha l & l < L_{LIM} \\ G_{MAX} & L_{LIM} < l < L_{MAX} \end{cases}$$

Results obtained applying RGE can be seen in Fig. 6: cracks on the lower edge are highlighted by applying the alignment (right) with respect to the original image (left).

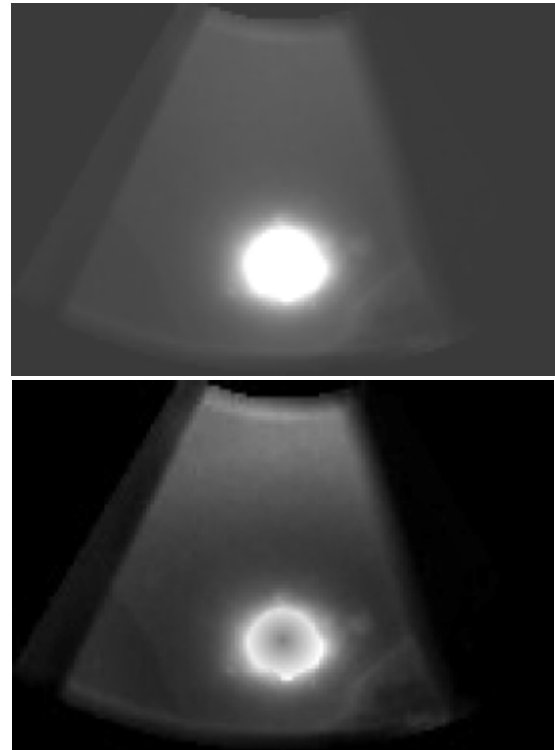


**Figure 3: Comparison gradient image before (left) and after (right) application of RGE.**

### Edge-Based Crack Detection

The proposed algorithm for the detection of cracks is designed to detect images of radial and tangential deficit, and has better performance when equalization is adopted. To detect cracks, gradient image is divided into smaller parts (patches) are identified separately. Each patch is binarized with adaptive threshold based on the average pixel value. Some image enhancing features are then applied, and finally cracks are detected select the outline of the image have a significant size, discarding the one containing the laser spot. The final algorithm for crack detection is fairly simple, since it operates in the images are strongly enhanced at a lower level.

Examples of crack detection can be seen in Fig. 7, where the binarized image is shown (left) together with the final result (right).

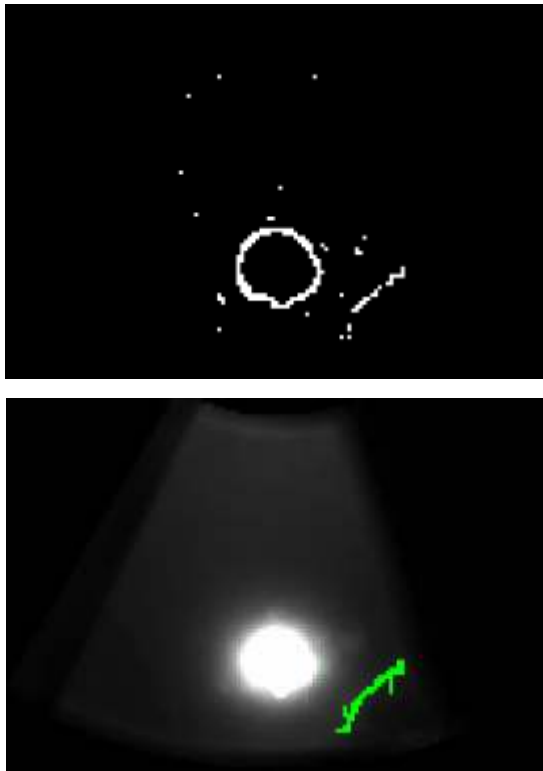


**Figure 4: Sample image binarization (left) and the final result (right) of the system**

### ANALYSIS OF RUGGED METAL PARTS

The algorithm described so far does not show a good performance in a rugged part, because detailed analyses of the radial and tangential mixing suffer from the noise generated by the rugged surfaces. A different

approach has been developed to deal with this issue, which is based on the radial density profile (RDP) [Kylberg et.al., 2011], a method that has been used to describe the medical images that contain viruses. Such medical images are rather similar case analysis laser spot as in both cases it is important to investigate the circular shape parts. RDP measures are used to train support vector machine [Theodoridis and Koutroumbas, 2009], which is a state-of-the-art including machine learning classifiers.

Although the algorithm described above can be regarded as "direct method", since it is designed to find form factors that shape crack, the method is based on RDP is "indirect" because it detects cracks analyze the evolution of the shape of the laser spot while it is heat crack. Heat source was not pulsated in this case, as it would be impossible to investigate features pulsating laser spot.

### DISCUSSION

The methods presented in this article have been tested on several rows. Test crack detection involved both single images and entire sequences.

In the case of smooth metal part, only few images that show a crack were present in the dataset, which was conducted on a limited number of pictures. Tests showed a good performance of the algorithm, which was able to detect cracks in the area around the laser spot. However, cracks can not be detected when they are too close to the laser spot itself, because it is masked by the algorithm, do something detection not possible. This means that in 38% of the shots crack is not identified, but the same crack was found before in other films, when it was located further from the laser spot. Considering all series, the algorithm showed optimal performance, because it discover all the cracks in the sequences, but the dataset is still too small to analyze the system.

Removal of crack sensor for rugged metal components was studied in more detail, thanks to a much larger dataset. The system was tested in 31 rows, each frame laser pass twice fissure; all series were taken with the same sample portion. The crack had very little dimension, having a length of 8:36 mm in length and width of 120 pm only.

The sequences are divided into two parts:

- The set A is the laser power is reduced to a given value of 7.5 W laser and the rate of change in the range of [60-200] mm / s, with a step of 10 mm / s between two rows in a row;
- In the B set speed is maintained at the value of 60 mm / s laser power takes a value in the range [5-20] W with step 1W.

As a testing protocol with the power go out one set protocol, that is, trained the categories of features extracted from the set of A and test it in a certain B, and vice versa. Tests resulted in an average area under the ROC curve 0.9337. The DET curve [Martin et al., 1997] is reported in Fig. 7, which shows the good performance achieved by the system, assuming that only one sample component bought changing laser power and scan speed was used for training and testing.

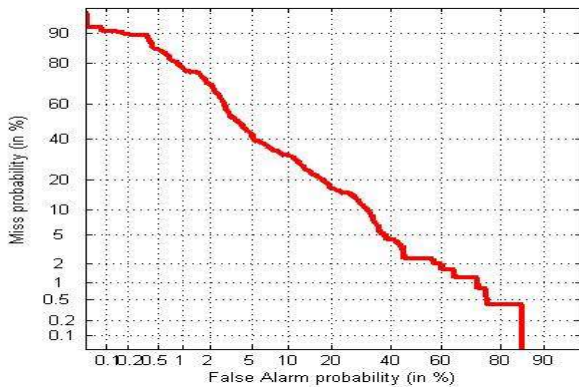


**Figure 5: DET curve for tests carried out on crack detection using RDP.**

**CONCLUSION**

In this article, a system for automatic discovery of cracks in metal parts was introduced. The system is based on thermographic analysis of the part under inspection and exploits laser excitation, either pulsed or continuous. The system utilizes different algorithms depending on the metal to view, which can be either smooth or rugged, and is able to detect cracks that are very small: the smallest found crack has a width of only 120 pm. Even though work is still ongoing, a first performance evaluation showed good results, indicating the approach is promising. Future work is the development of algorithms for thermographic image processing for detecting defects on a thermogram obtained by flash thermography.

**REFERENCES**

Gachagan A., McNab A. and Reynolds P., 2004. "Analysis of ultrasonic waves propagating in the metal pipe structures using finite element modeling technology." *Ultrasonics Symposium, IEEE*, **2**: 938-941, 204.

Theodoulidis T.P., Panas S.M. and Kriezis E.E., 1994. "Eddy current crack detection strategy using the elliptical stimulation," *Science, measurement and technology, IEE case*, **141**(1):41-47.

Xu P. and Shida K., 2008. "Eddy current sensor with a novel probes for crack detection position," *Industrial Technology, 2008. ICIT 2008 IEEE International Conference on*, pp.1-6, 21-24 April 2008 DOI: 10.1109 / ICIT.2008.4608445 .

Tian G.Y., Sophia A., Taylor D. and Rudl J., 2005. "multiple sensors on pulsed eddy-current detection for 3-D subsurface cracking food," *Sensors Journal, IEEE*, vol.5, No.1, pp .90-96, in February 2005. doi: 10.1109 / JSEN.2004.839129.

Hwang J., Kim J. and Lee J., 2009. "Magnetic pictures of the surface crack on heating the sample with an area-type magnetic camera with high spatial resolution," *instrumentation and measurement techniques Conference, 2009. I2MTC '09. IEEE*, pp.1546-1551, 5-7 May 2009.

Sophia A., Tian G.Y. and Zairi S., 2006. "pulsed magnetic flux leakage methods for crack detection and characterization", *sensors and actuators*, **125**(2):186-191, ISSN 0924-4247.

Liu T.J.C., 2010. "Application of Thermo-electric Joule heating for crack detection," *Mechanical and Electronics Engineering (ICMEE) 2010 2nd International Conference on*, Vol.1, pp.V1-103, V1-107, 1-3 August 2010. Doi : 10.1109 / ICMEE.2010.5558585.

Shafeek H.I., Gadelmawla E.S., Abdel-Shafy A.A. and Elewa I.M., 2004. "Evaluation of welding defects for gas pipeline radiographs using computer vision," *NDT & E International*, **37**(4):291-299, ISSN 0963-8695, 10.1016 / j.ndteint.2003.10.003.

- Prasanna P., Dana K., Gucunski N. and Basily B., 2012. "Computer vision-based crack detection and analysis." Proc. Spie 8345, sensors and Smart Structures Technologies for Civil, Mechanical and Aerospace Systems 2012 834 542 (26 April 2012); Doi: 10.1117 / 12.915384.
- Turakhia N., Shah R. and Joshi M., 2012. "Automatic crack detection in Heritage Site images for image inpainting," in Proceedings of the eighth Indian Conference on Computer Vision, Graphics and Image processing (ICVGIP '12). ACM, New York, NY, USA, Article 68. Doi: 10.1145 / 2425333.2425401
- Genest M., Dudzinski D.C., Bulmer S. and Kersey R.K., "Crack detection with activation of thermography for the thermo-mechanical fatigue testing", AIP Conf. Proc. 1335, pp 1727-1734. Doi: <http://dx.doi.org/10.1063/1.3592137>.
- Wagner D., Ranc N., Bathias C. and Paris P.C., 2010. "Fatigue crack initiated discovery of infrared thermography method", *Fatigue and Fracture of Engineering Materials & structures*, **33**(1).
- Kostson E., Weekes B., Almond D.P., Wilson J. and Tian G.Y., "Crack detection with eddy current pulsing stimulated thermography", AIP Conf. Proc. 1335, pp 415-422. Doi: <http://dx.doi.org/10.1063/1.3591882>.
- Maldague X., Galmiche F. and Ziad A., 2002. "Advances in pulsed phase thermography," *Infrared Physics & Technology*, **43**(3-5):175-181, ISSN 1350-4495, 10.1016 / S1350-4495 (02) 00138-X.
- T. Maffren P. Junca, F. and G. Lepoutre Debat, "Crack detection in high-pressure turbine blade with a flying spot function thermography swirl of range", AIP conf. Proc. 1430, pp 515-522. Doi: <http://dx.doi.org/10.1063/1.4716270>.
- Jacquey F., Comby F. and Strauss O., 2007. "Non-additive approach to omnidirectional image gradient opinion," *Computer Vision, 2007. ICCV 2007. IEEE 11th International Conference on*, pages 1-6, 2007.
- Kylberg G., Uppström M. and Sintorn I.M., 2011. "Virus Texture Analysis Using Local Binary Patterns and radial density profiles," in *proceeding 16 Iberoamericana Congress on pattern recognition (CIARP), LNCS-7042*, pp 573-580, Pucon, Chile, November 2011. DOI: 10.1007 / 978-3-642-25085-9\_68.
- Theodoridis S. and Koutroubas K., 2009. "pattern recognition", 4th Edition, Academic Press, ISBN 978-1-59749-272-0.
- Martin A., Doddington G., Kamm T., Ordowski M. and Przybocki M., 1997. "The DET Curve in assessing the perception of Task Performance", *Proc. Speech Euro '97, Rhodes, Greece*, **4**: 1899-1903.